



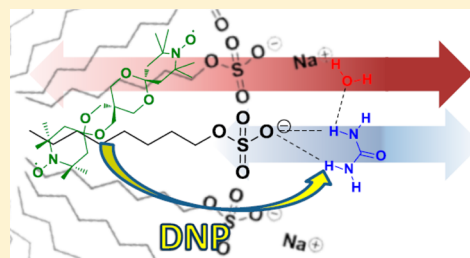
High Field Dynamic Nuclear Polarization NMR with Surfactant Sheltered Biradicals

Matthew K. Kiesewetter,[†] Vladimir K. Michaelis,^{†,‡} Joseph J. Walish,[†] Robert G. Griffin,^{*,†,‡} and Timothy M. Swager^{*,†}

[†]Department of Chemistry and [‡]Francis Bitter Magnet Laboratory, Massachusetts Institute of Technology, Cambridge, Massachusetts 02139, United States

S Supporting Information

ABSTRACT: We illustrate the ability to place a water-insoluble biradical, bTbk, into a glycerol/water matrix with the assistance of a surfactant, sodium octyl sulfate (SOS). This surfactant approach enables a previously water insoluble biradical, bTbk, with favorable electron–electron dipolar coupling to be used for dynamic nuclear polarization (DNP) nuclear magnetic resonance (NMR) experiments in frozen, glassy, aqueous media. Nuclear Overhauser enhancement (NOE) and paramagnetic relaxation enhancement (PRE) experiments are conducted to determine the distribution of urea and several biradicals within the SOS macromolecular assembly. We also demonstrate that SOS assemblies are an effective approach by which mixed biradicals are created through an assembly process.



INTRODUCTION

Nuclear magnetic resonance is the dominant spectroscopic tool for the characterization of most chemical systems. In particular, solid-state NMR (ssNMR) has shown promise in characterizing disordered biological complexes (e.g., membrane proteins and amyloid fibrils^{1,2}) which are inaccessible via traditional diffraction-based methods. However, the success of these experiments is often limited due to the low Boltzmann polarization of nuclear spins, leading to extended acquisition times (i.e., >weeks).³ High field dynamic nuclear polarization (DNP) is an approach that dramatically increases the sensitivity of NMR experiments.^{4–6} Specifically, DNP can hyperpolarize NMR-active nuclei, yielding a gain in sensitivity of 2–3 orders of magnitude. High-field DNP involves transferring electron polarization to nuclei via one of several possible mechanisms upon microwave irradiation of the electron EPR transitions.⁷ Although DNP was conceptually conceived and demonstrated in the 1950s,⁴ a renaissance in the methodology has occurred in the past few years. This is due largely to the development of high-power microwave sources (i.e., gyrotrons) and improvements in instrumentation (i.e., cryogenics and MAS probe technology) required to conduct these experiments at high fields (>5 T), and this has served as a major driving force for the commercialization of DNP instrumentation.^{8–11} A second and equally critical component of this methodology is access to stable radicals from which the polarization is ultimately derived.

The DNP mechanism judged to be most efficient in high-field DNP NMR experiments is the cross effect (CE) mechanism,^{12–14} whereby hyperpolarization occurs through a three-spin “flip–flop–flip” process involving two electrons and a nucleus.^{12–15} The dominant mechanism in a given experiment is determined in part by the relative magnitudes of the

electron homogeneous (δ) and inhomogeneous (Δ) line widths and the nuclear Larmor frequency (ω_{01}). The CE is dominant when the polarizing agents satisfy, $\Delta > \omega_{01} > \delta$, as is the case for nitroxide containing radicals. Fine-tuning the resonance frequencies of the two electrons to match the nuclear Larmor frequency optimizes the signal enhancement, ϵ , that is achievable, $\epsilon_{\max} \approx 660 (\gamma_e/\gamma_H)$ for ^1H .¹⁶ The electron–electron coupling and frequency separation can be altered in practice by synthetically modulating the relative orientation and interelectron distance, an approach that has been the mainstay of biradical design for the past decade.^{14,17–20} For example, the molecule bTbk (Scheme 1) ostensibly has a superior geometry and electron–electron dipolar coupling as compared to TOTAPOL but lacks solubility in biological friendly solvents. SPIROPOL has superior solubility to bTbk but has decreased dipolar electron coupling. Very recently, Tordo and co-workers introduced two new radicals based on BTurea, and Pypol and AMUpol display very promising gains in sensitivity for ^1H DNP NMR, at temperatures between 100 and 160 K.²¹

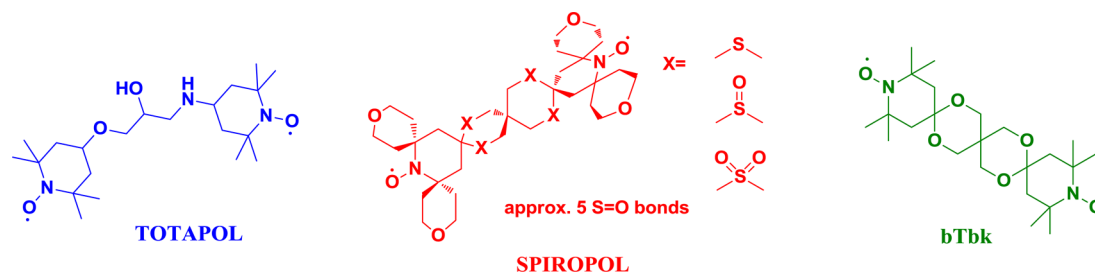
Interest in applying DNP to the investigations of biological materials, where NMR signal intensity is of extreme importance, has solidified glycerol/water as a dominant medium for DNP experiments.²² Glycerol/water mixtures have the dual benefit of being suitable for biological samples and forming a solid glass regardless of cooling rate.^{23,24} Glass formation is particularly important to ensure a homogeneous distribution of the polarizing agent, the inhibition of ice formation to prevent protein denaturation at cryogenic

Received: October 21, 2013

Revised: January 28, 2014

Published: February 7, 2014

Scheme 1. Nitroxide Biradicals TOTAPOL (Blue), SPIROPOL (Red), and bTbk (Green)



temperatures (i.e., <110 K), and the promotion of effective spin-diffusion to rapidly transfer polarization throughout the sample.^{19,23} Accordingly, the pursuit of biradicals has primarily been limited to those that are soluble in glycerol/water mixtures. This limitation can be particularly frustrating when ostensibly superior polarization agents can be conceived and synthesized but are insoluble in glycerol/water.^{18,20,25,26} For example, after the report of bTbk,²⁷ a polarization agent with a ϵ superior to TOTAPOL in DMSO/water, several years lapsed in an effort to reproduce the enhancements in aqueous solvent, efforts that were only partially successful in the advent of SPIROPOL.¹⁷

The use of surfactants is a common, cost-effective, method to dissolve organic compounds in aqueous environments,^{28–30} yet this approach has not been employed for the dissolution of polarization agents in water. In this communication, we illustrate the ability to place water-insoluble bTbk into a glycerol/water matrix with the assistance of a surfactant. This surfactant approach adds bTbk as well as other water-insoluble radicals to the armamentarium of biradicals available for aqueous DNP. Further, we explore a common solvent system in order to benchmark all (bi)radicals, even water-insoluble radicals, against each other.

EXPERIMENTAL SECTION

Isotopically enriched urea-¹³C (99% ¹³C) and D₂O (99%) were purchased from Cambridge Isotope Laboratories (Andover, MA, USA). Sodium octyl sulfate-*d*₁₇ was purchased from CDN (Pointe-Claire, Quebec, Canada), and glycerol-*d*₈ (98% ²H) was purchased from DyNuPol, Inc. (Newton, MA, USA). The biradicals SPIROPOL and bTbk were prepared according to published procedures,^{17,18} while TOTAPOL¹⁹ was purchased from DyNuPol. The monoradical Finland trityl was purchased from GE Healthcare. All other materials were obtained from Sigma-Aldrich. All chemicals were used as received.

Sample Preparation. Samples were prepared in air by weighing solids directly into a glass vial. Solvent was added to solids which were dissolved with gentle heating and agitation, if necessary. Samples were never subjected to sonication, as it leads to rapid degradation of the nitroxide moiety.³¹ Samples were then transferred to either NMR tubes (solution studies) or sapphire rotors (solid state DNP studies) as applicable.

Nuclear Overhauser Effect (NOE) Experiments. NOE experiments were performed on a Varian 400 MHz spectrometer using the NOE difference macro in VNMR with the following parameters: acquisition time = 3.0 s; preacquisition delay = 10 s; pulse width = 9.0 ms; pulse power = 60 dB; steady state scans = 2; decoupling nucleus = ¹H; saturation delay = 5 s; number of transients = 64; saturation power = 15 dB (HOD), 5 dB (urea); reference saturation frequency = 5000 Hz.

Paramagnetic Relaxation Enhancement (PRE) Experiments. Four NMR samples were made containing urea-¹³C (1 M) and SOS (0.75 M, SOS-H) in glycerol-*d*₈/D₂O/H₂O (0.3 mL; 60/30/10) with either no radical or 10 mM bTbk, TOTAPOL, or SPIROPOL. Into each of these NMR samples, a sealed glass capillary tube containing 10% C₆H₆ in C₆D₆ was inserted; the C₆H₆ ¹H NMR resonance is free of PRE under all conditions and serves as an internal standard. A well-shimmed ¹H NMR experiment was acquired for each sample. The line width of a resonance ($\Delta\omega_{pp}$) is proportional to the nuclear transverse relaxation rate. The presence of a paramagnet shortens T_2 and enhances the relaxation rate, R_2 , where the line width provides a direct readout of R_2^* , the observed relaxation rate, $R_2^* = \Delta\omega_{pp}\pi = 1/T_2^*$. The intrinsic line width of each resonance was taken to be those of the paramagnet-free sample ($\Delta\omega_{pp}\pi = R_2$), and the observed line width in the paramagnetic samples, $\Delta\omega_{pp}\pi = R_2^* = 1/T_2^*$, is the difference from the intrinsic line width caused by the PRE (i.e., the spin–paramagnet interactions),^{32–34} $PRE = R_2^{sp} = R_2^* - R_2$.

Solubility Measurements. The solubility of the three biradicals was determined by serial addition of material or dilution with the appropriate solvent system. For example, bTbk (10.0 mg; 10 mM) was added to 2.5 mL of glycerol-*d*₈/D₂O/H₂O (60/30/10) and stirred with gentle heating (50 °C). After 30 min, precipitate persisted, and the concentration of bTbk was reduced by half by the addition of solvent. The solution was stirred and heated for 30 min, and this heating/stirring/dilution process was repeated until the failure of the 1 mM solubility experiment. For SPIROPOL and TOTAPOL, the serial additions of material were concluded (in 10 mM increments, followed by 1 mM increments) if precipitate remained after 30 min of heating and stirring.

Dynamic Nuclear Polarization NMR Measurements. Dynamic nuclear polarization magic-angle spinning NMR experiments were performed on a home-built spectrometer, consisting of a 212 MHz (¹H, 5 T) NMR magnet (courtesy of Dr. David Ruben, FBML, MIT) and a 139.65 GHz cyclotron resonance maser (i.e., gyrotron) generating high-power microwaves up to 14 W. MAS NMR spectra were recorded on a home-built cryogenic 4 mm quadrupole resonance (¹H, ¹³C, ¹⁵N, and e[−]) DNP NMR probe equipped with a Kel-F stator (Revolution NMR, Fort Collins, CO). Microwaves are guided to the sample via a circular overmoded waveguide whose inner surface has been corrugated to reduce mode conversion and ohmic losses. Sample temperatures were maintained at 83 (±1) K, with a spinning frequency, $\omega_r/2\pi = 4.0$ kHz. ¹³C{¹H} cross-polarization³⁵ experiments using a 1.5 ms contact time were acquired under continuous microwave irradiation. Sample temperatures were measured using a Neoptix (Quebec, Canada) thermocouple which were calibrated between 3 and 353 K. High-power TPPM³⁶ proton decoupling (¹H $\gamma B_1/2\pi =$

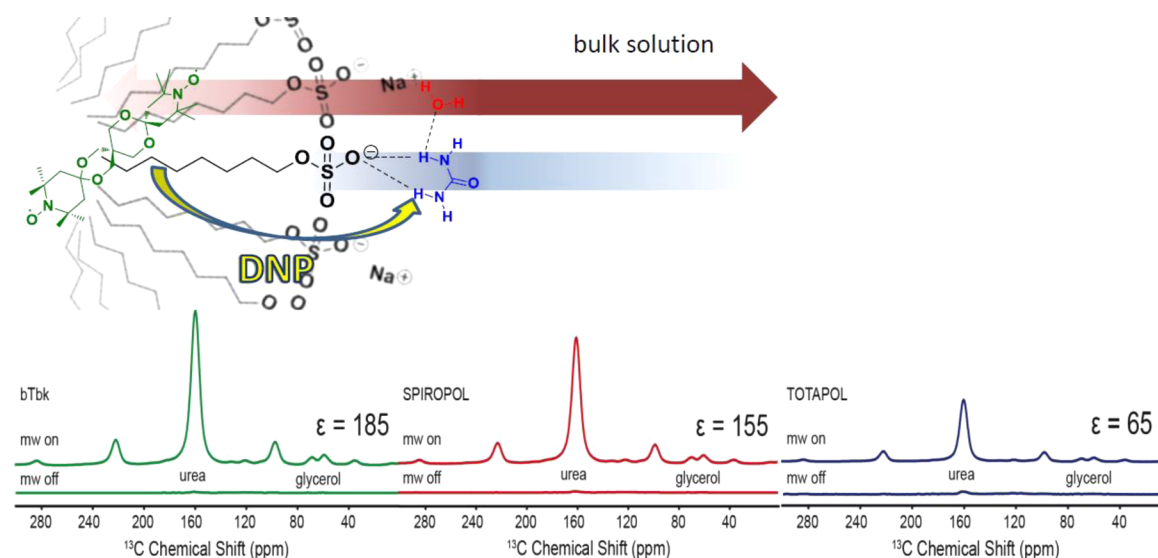


Figure 1. (upper) NOE and PRE data suggest that bTbk is isolated within the SOS assembly but is dipole coupled via ^1H spin diffusion with the urea, localized near the exterior of the assembly. NOE data suggest that water/glycerol solvation is strongest on the exterior of the SOS assembly but does extend to the core. (bottom) The (CP) MAS DNP enhancement exhibited by bTbk, SPIROPOL, and TOTAPOL in glycerol- d_8 /D $_2$ O/H $_2$ O (v/v/v 60/30/10) solvent mixtures (containing 1 M urea- ^{13}C and 0.75 M SOS (SOS- d_{17} /SOS-H = 95/5)).

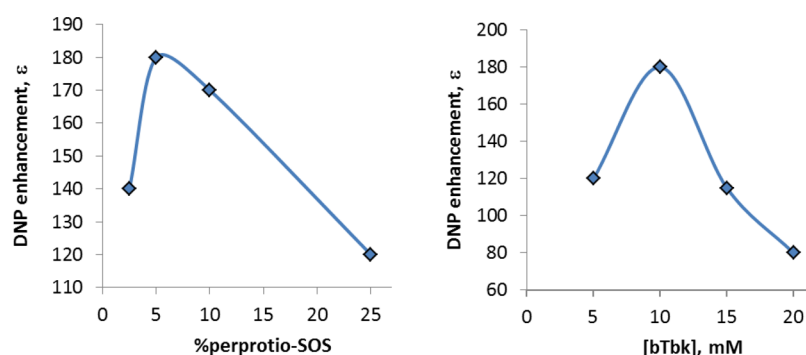


Figure 2. $^{13}\text{C}\{^1\text{H}\}$ CPMAS DNP NMR enhancements of 1 M urea- ^{13}C in glycerol- d_8 /D $_2$ O/H $_2$ O (v/v/v 60/30/10) varying the % H SOS (left) with 10 mM bTbk and [bTbk] (right) at 0.75 M SOS (5% H). The lines are a guide for visualization of the trends.

100 kHz) was used during acquisition. Buildup times (T_B) were determined using a saturation recovery experiment. The recycle delay was chosen as $T_B \times 1.3$, yielding optimum sensitivity per unit of time. Microwave power was kept constant at 8 W using a PID control interfaced within Labview. ^1H cross-effect conditions were optimized for each radical by sweeping the main NMR field using a ± 750 G sweep coil in order to sit at the maximum positive enhancement position within the DNP field profiles.^{17,19,27} Samples were contained in 4 mm sapphire rotors equipped with a Vespel drive tip and Kel-F spacer.

RESULTS AND DISCUSSION

bTbk is only soluble in glycerol/water solution upon the addition of surfactant. Addition of sodium octyl sulfate (SOS; 0.57 M) to a glycerol- d_8 /D $_2$ O/H $_2$ O (v/v/v 60/30/10)³⁷ solution of urea (1 M) containing precipitated bTbk (10 mM) followed by agitation, and gentle heating produces a stable yellow-orange homogeneous solution. The addition of the SOS does not visually disrupt the glass formation of the solvent system. Solubility testing reveals bTbk is not soluble with SOS concentrations below 0.57 M.

The intermolecular nuclear Overhauser effect (NOE) is a powerful tool for characterizing a complex solution. In an NMR

tube containing 1 M urea and SOS (0.75 M) in glycerol- d_8 /D $_2$ O/H $_2$ O (v/v/v 60/30/10), an NOE experiment irradiating the water/glycerol peak at maximum power provides an indication of solvent exposure of the species in solution. Intermolecular NOEs are difficult to quantify between species especially in an incomplete saturation situation, but the NOE from the solvent to the urea is approximately 10 \times the enhancement observed in the same solution from the solvent to SOS. Further, the NOEs extend across the entire SOS alkyl chain, with each internal methylene and the methyl resonance experiencing an NOE approximately 0.25 \times the methylene α to the sulfate moiety. In a separate experiment where the urea peak is saturated, the NOE appears only on the water/glycerol resonances with no detectable NOE from the urea to the SOS. Taken together, these observations suggest that urea resides mainly in the bulk solvent, but the water/glycerol solvation extends to the core of the SOS macromolecular structure.

The short- to medium-range distance (< 6 Å)³⁴ information available from NOE experiments can be complemented with paramagnetic relaxation enhancement (PRE) measurements whose effects extend upward of 25 Å.³⁸ Indeed, simple ^1H NMR spectra of bTbk/SOS solutions compared to a paramagnet-free SOS-containing solution indicate the preferred

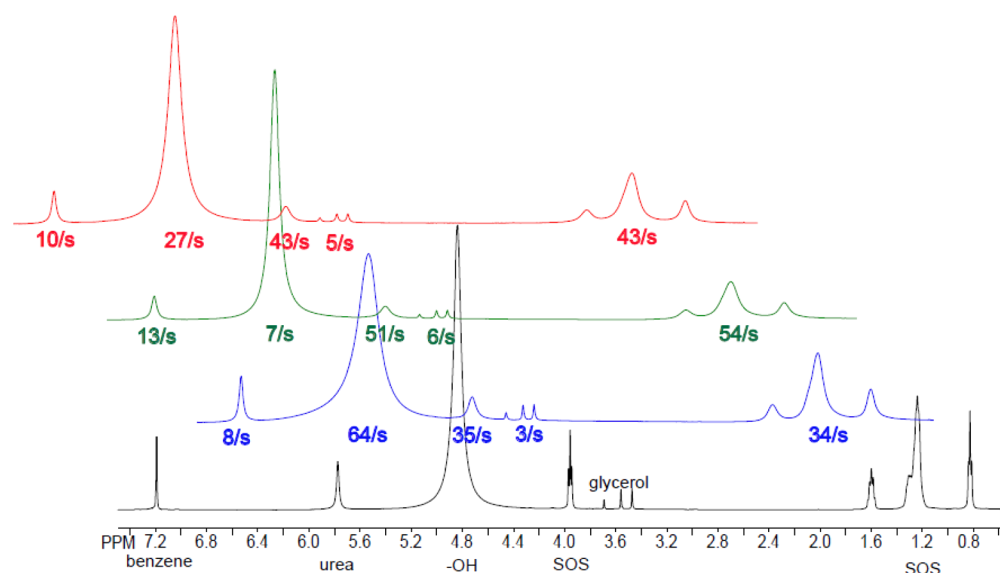


Figure 3. ^1H NMR spectra of 1 M urea and 0.57 M SOS-H in glycerol/ $\text{D}_2\text{O}/\text{H}_2\text{O}$ (60/30/10) with (black) no radicals present, (blue) 10 mM TOTAPOL, (green) 10 mM bTbk, and (red) 10 mM SPIROPOL. The PRE is given below each resonance.

location of the biradical in solution. The NMR line widths are proportional to the nuclear spin–spin relaxation time constant, T_2 via the Solomon equation,³³ and altering the nuclear T_2 by paramagnetic relaxation changes the line width, thereby providing a direct readout of the proximity of the biradical. A sealed glass capillary of benzene in benzene- d_6 provides an internal standard that is free from PRE under all conditions. Our PRE experiments suggest that bTbk preferentially occupies the interior of the SOS assembly and is uniformly relaxing the SOS methylene moieties. Despite being localized in the interior SOS macromolecular structure, bTbk exhibits PRE to the urea ($\text{PRE}_{\text{urea}} = 13.3 \text{ s}^{-1}$, see the Experimental Section). This is in stark contrast to the NOE results and suggests that, while the bTbk and urea are located in separate components of the solution, they are in sufficient contact via electron–nuclear dipole couplings to provide for effective DNP enhancements, Figure 1.³⁹ Remarkably, the PRE for the HOD solvent is smaller than that to the urea ($\text{PRE}_{\text{HOD}} = 6.9 \text{ s}^{-1}$, by a factor of $\sim 20\times$ difference considering $[\text{HOD}] \sim 20[\text{urea-H}_1]$, post H/D exchange). Such a difference suggests that the urea may be localized near the SOS assembly exterior, perhaps due to favorable H-bonding. Nonetheless, PRE_{HOD} is present, which facilitates spin diffusion throughout the sample.

A screen of the conditions was conducted to maximize the ^{13}C cross-polarization (CP) MAS DNP enhancement of urea- ^{13}C as derived from bTbk in glycerol/water. The maximum signal enhancement of $\epsilon = 185$ obtained in 1 M urea- ^{13}C in glycerol- $d_8/\text{D}_2\text{O}/\text{H}_2\text{O}$ (v/v/v 60/30/10) was found at 5% SOS-H (SOS- $d_{17}/\text{SOS-H} = 95/5$) and $[\text{bTbk}] = 10 \text{ mM}$. The results in Figure 2, are in agreement with the required $^1\text{H}/^2\text{H}$ ratio as well as biradical concentration using traditional water-soluble biradicals.¹⁹ The screening was performed at $[\text{SOS}]_{\text{total}} = 0.75 \text{ M}$, but ϵ was identical at $[\text{SOS}]_{\text{total}} = 0.57 \text{ M}$, which was the minimum required $[\text{SOS}]_{\text{total}}$ to dissolve the 10 mM bTbk. A surfactant concentration of 0.57 M SOS was used in all subsequent experiments. The ϵ was then measured for other biradicals at 10 mM biradical and 0.57 M SOS (5% H): $\epsilon_{\text{SPIROPOL}} = 155$ and $\epsilon_{\text{TOTAPOL}} = 65$; see the Supporting Information. The difference in ϵ for bTbk and SPIROPOL is similar ($(185 - 155)/185 \sim$

17%) to that measured across different solvent platforms.^{17,18} The surprising measurement is the ϵ for TOTAPOL, which when measured under identical conditions free of SOS is $\epsilon = 160$. These and all enhancements within the manuscript were measured from the urea- ^{13}C resonance; however, the glycerol enhancements were within experimental error of the urea- ^{13}C signal. This indicates that efficient electron- ^1H communication and ^1H – ^1H spin-diffusion effectively transfer a global ^1H enhancement across the whole system.

The PRE experiment was repeated using TOTAPOL and SPIROPOL, and these results are shown in Figure 3. The trend of biradical PRE to the solvent –OH resonance is proportional to the solubility of the biradicals in glycerol/water mixtures without SOS: TOTAPOL is highly soluble ($\sim 50 \text{ mM}$), SPIROPOL is moderately soluble ($\sim 10 \text{ mM}$), and bTbk is insoluble ($\ll 1 \text{ mM}$). Accordingly, the magnitude of the PRE on the SOS resonances runs inversely with biradical solubility as does the PRE_{urea} due to each biradical. This observation is also consistent with a simple solubility argument. If the urea is highly associated with the micelle, as the PRE observations suggest, then the biradical that is most soluble in the reaction media (i.e., those that do not need SOS to become soluble) will have the least contact with the urea and exhibit the smallest enhancement. This observation could be used to inform the DNP NMR studies upon complicated samples. For example, the choice of biradical would be prudent when one wishes to study cell membranes versus intra/extra-cellular environment.

The synthetic generation of heterobiradicals (cf. BDPA-TEMPO biradicals) has been the thrust of our research effort.²⁵ Although this area of research has tremendous potential, we posited that the hydrophobic environment at the interior of the SOS macromolecular structure might allow for the self-assembly of such biradicals. Toward this end, we examined the solubility of several monoradicals in 0.75 M SOS: BDPA, alkyl-derivatized BDPAs, and trityl radical were all insoluble. Finland trityl, a more hydrophilic version of the parent trityl radical, was adequately soluble. DNP of urea in 0.57 M SOS (5% H) with 10 mM Finland trityl and 10 mM TEMPO in the usual solvent mixture gave $\epsilon = 70$; see the Supporting Information (all enhancements reported for the SOS system

are collected in Table 1). This is approximately the same ϵ measured for 10 mM TEMPO and 10 mM Finland trityl in free

Table 1. CP-MAS DNP Enhancements and Buildup Times for the Examined (Bi)radicals^a

radical	T_1/T_B (s)	^1H enhancement (ϵ)
TOTAPOL	6.2	65
SPIROPOL	8.9	155
bTbK	4.8	185
Finland trityl/TEMPO ^b	5	70

^a1 M urea- ^{13}C in glycerol- d_8 /D $_2$ O/H $_2$ O (v/v/v 60/30/10), 0.57 M SOS (SOS- d_{17} /SOS-H = 95/5), and 10 mM biradical. ^b10 mM of each radical.

solution.¹⁰ The remarkable difference is in the buildup times for the mixed biradical: 5 s with SOS vs 10.5 s without SOS. This shorter buildup time allows for an experimental recycling delay to be reduced by a factor of 2 compared to the system without SOS. The average electron–electron dipolar coupling for the three biradicals *vide supra* is between 25 and 30 MHz, whereas a 20 mM (10 mM/10 mM) mixed monoradical is ~ 0.6 MHz. Initial studies using the mixed monoradical approach for direct DNP of ^1H ($T_B \sim 5$ s)¹⁴ and ^{13}C in free solution utilized a 40 mM electron concentration (twice the molar concentration) for effective DNP enhancements with a dipolar coupling being ~ 1.2 MHz.⁴⁰ The reduced buildup time constant observed is consistent with a stronger electron–electron dipolar coupling caused by the proximity of the monoradicals trapped within the surfactant. A thorough screening of self-assembled mixed biradicals and the origin of the attenuated buildup time will be explored in the future.

CONCLUSION

The addition of a surfactant, sodium octyl sulfate, to glycerol/water solutions allows for the acquisition of DNP data for classically water-insoluble radicals. This approach allows for the first time the comparative testing of three biradical polarization agents in a side-by-side manner. The stark attenuation of the DNP enhancement of TOTAPOL in SOS-containing glycerol/water suggests that this bis-nitroxide may not be the best biradical for surfactant-like situations, including cell membranes. Further, judicious choice of the biradical could allow, for example, selective enhancement of membrane proteins without paramagnetic relaxation. The possibility of rapidly screening mixed biradicals, like the Finland trityl/TEMPO system, is an exciting advance for polarization agent synthesis and may guide future synthetic efforts. Indeed, the outlook for surfactant encapsulated radical DNP on various chemical systems seems promising, with the recent paper by Mao et al. using a similar approach with cyclodextrin.⁴¹ Combined with the wide array of mono- and biradicals available,^{17,18,20,21,40,42} this approach should offer effective methods to polarize important chemical systems opening up new scientific avenues.

ASSOCIATED CONTENT

Supporting Information

Tables showing CP-MAS DNP enhancements, buildup times, and inter-radical distances of the biradicals used in this study and CP-MAS DNP enhancements and buildup times for the various concentrations of bTbK studied. Figures showing CP-MAS DNP, ^1H -NMR, and ^1H NOE difference NMR spectra.

This material is available free of charge via the Internet at <http://pubs.acs.org>.

AUTHOR INFORMATION

Notes

The authors declare no competing financial interest.

ACKNOWLEDGMENTS

The research reported in this publication was supported by the National Institute of Biomedical Imaging and Bioengineering of the National Institutes of Health under Awards EB-002804, EB-002026, EB-001960, and GM-095843. V.K.M. is grateful to the Natural Sciences and Engineering Research Council of Canada for a postdoctoral fellowship. M.K.K. would like to thank the National Institute of Biomedical Imaging and Bioengineering for a NRSA Fellowship (F32EB012937).

REFERENCES

- (1) Fitzpatrick, A. W. P.; Debelouchina, G. T.; Bayro, M. J.; Clare, D. K.; Caporini, M. A.; Bajaj, V. S.; Jaroniec, C. P.; Wang, L.; Ladizhansky, V.; et al. Atomic Structure and Hierarchical Assembly of a Cross- β Amyloid Fibril. *Proc. Natl. Acad. Sci. U.S.A.* **2013**, *110*, 5468–5473.
- (2) Debelouchina, G. T.; Platt, G. W.; Bayro, M. J.; Radford, S. E.; Griffin, R. G. Intermolecular Alignment in Amyloid Fibrils. *J. Am. Chem. Soc.* **2010**, *132*, 17077–17079.
- (3) Dobson, C. M. Protein Misfolding, Evolution and Disease. *Trends Biochem. Sci.* **1999**, *24*, 329–332.
- (4) Overhauser, A. W. Polarization of Nuclei in Metals. *Phys. Rev.* **1953**, *92*, 411–415.
- (5) Slichter, C. P. The Discovery and Demonstration of Dynamic Nuclear Polarization - A Personal and Historical Account. *Phys. Chem. Chem. Phys.* **2010**, *12*, 5741–5751.
- (6) Carver, T. R.; Slichter, C. P. Polarization of Nuclear Spins in Metals. *Phys. Rev.* **1953**, *92*, 212–213.
- (7) Farrar, C. T.; Hall, D. A.; Gerfen, G. J.; Inati, S. J.; Griffin, R. G. Mechanism of Dynamic Nuclear Polarization in High Magnetic Fields. *J. Chem. Phys.* **2001**, *114*, 4922–4925.
- (8) Bajaj, V.; Farrar, C. T.; Hornstein, M. K.; Mastovsky, I.; Vieregg, J.; Bryant, J. A.; Elena, B.; Kreischer, K. E.; Temkin, R. J.; Griffin, R. G. Dynamic Nuclear Polarization at 9T Using a Novel 250 GHz Gyrotron Microwave Source. *J. Magn. Reson.* **2003**, *160*, 85–90.
- (9) Barnes, A. B.; Markhasin, E.; Daviso, E.; Michaelis, V. K.; Nanni, E.; Jawla, S. K.; Mena, E. L.; DeRocher, R.; Thakkar, A.; Woskov, et al. Dynamic Nuclear Polarization at 700 MHz/460 GHz. *J. Magn. Reson.* **2012**, *224*, 1–7.
- (10) Griffin, R. G.; Prisner, T. F.; Hunter, R. I.; Cruickshank, P. A. S.; Bolton, D. R.; Riedi, P. C.; Smith, G. M.; Chem, P. C.; Kryukov, E. V.; et al. Solid-state Dynamic Nuclear Polarization at 263 GHz: Spectrometer Design and Experimental Results. *Phys. Chem. Chem. Phys.* **2010**, *12*, 5850–5860.
- (11) Bayro, M. J.; Debelouchina, G. T.; Eddy, M. T.; Birkett, N. R.; Macphee, C. E.; Rosay, M. M.; Maas, W. E.; Dobson, C. M.; Griffin, R. G. Intermolecular Structure Determination of Amyloid Fibrils with Magic-Angle Spinning and Dynamic Nuclear Polarization NMR. *J. Am. Chem. Soc.* **2011**, *133*, 13967–13974.
- (12) Hwang, C. F.; Hill, D. A. Phenomenological Model for the New Effect in Dynamic Polarization. *Phys. Rev. Lett.* **1967**, *19*, 1011–1013.
- (13) Hwang, C. F.; Hill, D. A. New Effect in Dynamic Polarization. *Phys. Rev. Lett.* **1967**, *18*, 110–111.
- (14) Hu, K.-N.; Song, C.; Yu, H.; Swager, T. M.; Griffin, R. G. High Frequency Dynamic Nuclear Polarization Using Biradicals: A Multi-frequency EPR Lineshape Analysis. *J. Chem. Phys.* **2008**, *128*, 052302–052312.
- (15) Wollan, D. S. Dynamic Nuclear Polarization with an Inhomogeneously Broadened ESR Line 2. Experiment. *Phys. Rev. B* **1976**, *13*, 3686–3696.

- (16) Griffin, R. G.; Prisner, T. F. High Field Dynamic Nuclear Polarization - The Renaissance. *Phys. Chem. Chem. Phys.* **2010**, *12*, 5737–5740.
- (17) Kiesewetter, M. K.; Corzilius, B.; Smith, A. A.; Griffin, R. G.; Swager, T. M. Dynamic Nuclear Polarization with a Water-Soluble Rigid Biradical. *J. Am. Chem. Soc.* **2012**, *134*, 4537–4540.
- (18) Matsuki, Y.; Maly, T.; Ouari, O.; Karoui, H.; Le Moigne, F.; Rizzato, E.; Lyubenova, S.; Herzfeld, J.; Prisner, T.; et al. Dynamic Nuclear Polarization with a Rigid Biradical. *Angew. Chem., Int. Ed. Engl.* **2009**, *48*, 4996–5000.
- (19) Song, C.; Hu, K.-N.; Joo, C.-G.; Swager, T. M.; Griffin, R. G. TOTAPOL: A Biradical Polarizing Agent for Dynamic Nuclear Polarization Experiments in Aqueous Media. *J. Am. Chem. Soc.* **2006**, *128*, 11385–11390.
- (20) Dane, E. L.; Corzilius, B.; Rizzato, E.; Stocker, P.; Maly, T.; Smith, A. A.; Griffin, R. G.; Ouari, O.; Tordo, P.; Swager, T. M. Rigid Orthogonal bis-TEMPO Biradicals with Improved Solubility for Dynamic Nuclear Polarization. *J. Org. Chem.* **2012**, *77*, 1789–1917.
- (21) Sauvée, C.; Rosay, M.; Casano, G.; Aussenac, F.; Weber, R. T.; Ouari, O.; Tordo, P. Highly Efficient, Water-Soluble Polarizing Agents for Dynamic Nuclear Polarization at High Frequency. *Angew. Chem., Int. Ed.* **2013**, *52*, 10858–10861.
- (22) Rienstra, C. M.; Hohwy, M.; Hong, M.; Griffin, R. G. 2D and 3D 15 N- 13 C- 13 C NMR Chemical Shift Correlation Spectroscopy of Solids: Assignment of MAS Spectra of Peptides. *J. Am. Chem. Soc.* **2000**, *122*, 10979–10990.
- (23) Baudot, A.; Alger, L.; Boutron, P. Glass-Forming Tendency in the System Water–Dimethyl Sulfoxide. *Cryobiology* **2000**, *40*, 151–155.
- (24) Iijima, T. Thermal Analysis of Cryoprotective Solutions for Red Blood Cells. *Cryobiology* **1998**, *36*, 165–173.
- (25) Dane, E. L.; Maly, T.; Debelouchina, G. T.; Griffin, R. G.; Swager, T. M. Synthesis of a BDPA-TEMPO biradical. *Org. Lett.* **2009**, *11*, 1871–1874.
- (26) Ong, T.-C.; Mak-Jurkauskas, M. L.; Walish, J. J.; Michaelis, V. K.; Corzilius, B.; Smith, A. A.; Clausen, A. M.; Cheetham, J. C.; Swager, T. M.; Griffin, R. G. Solvent-Free Dynamic Nuclear Polarization of Amorphous and Crystalline ortho-Terphenyl. *J. Phys. Chem. B* **2013**, *117*, 3040–3046.
- (27) Matsuki, Y.; Maly, T.; Ouari, O.; Karoui, H.; Le Moigne, F.; Rizzato, E.; Lyubenova, S.; Herzfeld, J.; Prisner, T.; et al. Dynamic Nuclear Polarization with a Rigid Biradical. *Angew. Chem., Int. Ed. Engl.* **2009**, *48*, 4996–5000.
- (28) Chang, J. The Structure of Sodium Dodecyl Sulfate Micelles in Solutions of H₂O and D₂O. *J. Phys. Chem.* **1985**, *89*, 2996–3000.
- (29) Gerig, J. T. Solute-Solvent Interactions Probed by Intermolecular NOEs. *J. Org. Chem.* **2003**, *68*, 5244–5248.
- (30) Ogino, K.; Nakamae, M.; Abe, M. Properties and Structure of Microemulsions. *J. Phys. Chem.* **1989**, *93*, 3704–3710.
- (31) Kirschenbaum, L. J.; Riesz, P. Sonochemical Degradation of Cyclic Nitroxides in Aqueous Solution. *Ultrason. Sonochem.* **2012**, *19*, 1114–1119.
- (32) Battiste, J. L.; Wagner, G. Utilization of Site-Directed Spin Labeling and High-Resolution Heteronuclear Nuclear Magnetic Resonance for Global Fold Determination of Large Proteins with Limited Nuclear Overhauser Effect Data. *Biochemistry* **2000**, *39*, 5355–5365.
- (33) Solomon, I. Relaxation Processes in a System of Two Spins. *Phys. Rev.* **1955**, *99*, 559–566.
- (34) Jahnke, W. Spin Labels as a Tool to Identify and Characterize Protein-Ligand Interactions by NMR Spectroscopy. *ChemBioChem* **2002**, *3*, 167–173.
- (35) Pines, A.; Gibby, M. G.; Waugh, J. S. Proton Enhanced Nuclear Induction Spectroscopy. A Method for High Resolution NMR of Dilute Spins in Solids. *J. Chem. Phys.* **1972**, *56*, 1776–1777.
- (36) Bennett, A. E.; Rienstra, C. M.; Auger, M.; Lakshmi, K. V.; Griffin, R. G. Heteronuclear Decoupling in Rotating Solids. *J. Chem. Phys.* **1995**, *103*, 6951–6955.
- (37) Ruiz, C. C.; Díaz-López, L.; Aguiar, J. Micellization of Sodium Dodecyl Sulfate in Glycerol Aqueous Mixtures. *J. Dispersion Sci. Technol.* **2008**, *29*, 266–273.
- (38) Gillespie, J. R.; Shortle, D. Characterization of Long-Range Structure in the Denatured State of Staphylococcal Nuclease. II. Distance Restraints from Paramagnetic Relaxation and Calculation of an Ensemble of Structures. *J. Mol. Biol.* **1997**, *268*, 170–84.
- (39) Smith, A. A.; Corzilius, B.; Barnes, A. B.; Maly, T.; Griffin, R. G. Solid Effect Dynamic Nuclear Polarization and Polarization Pathways. *J. Chem. Phys.* **2012**, *136*, 015101–015111.
- (40) Michaelis, V. K.; Smith, A. A.; Corzilius, B.; Haze, O.; Swager, T. M.; Griffin, R. G. High-Field 13C Dynamic Nuclear Polarization with a Radical Mixture. *J. Am. Chem. Soc.* **2013**, *135*, 2935–2938.
- (41) Mao, J.; Akhmetzyanov, D.; Ouari, O.; Denysenkov, V.; Corzilius, B.; Plackmeyer, J.; Tordo, P.; Prisner, T. F.; Glaubitz, C. Host-Guest Complexes as Water-Soluble High-Performance DNP Polarizing Agents. *J. Am. Chem. Soc.* **2013**, *135*, 19275–19281.
- (42) Maly, T.; Miller, A.-F.; Griffin, R. G. In Situ High-Field Dynamic Nuclear Polarization—Direct and Indirect Polarization of 13C Nuclei. *ChemPhysChem* **2010**, *11*, 999–1001.